Energy Yield Modeling of Perovskite–Silicon Tandem Photovoltaics: Degradation and Total Lifetime Energy Yield

Seyedamir Orooji and Ulrich W. Paetzold*

This study investigates the impact of degradation in perovskite-silicon tandem solar cells by means of energy yield (EY) modelling over the entire lifetime. First, we assess the impact on EY of degradation in the individual solar cell parameters of the perovskite top cell. Our analysis reveals that degradation in fill factor, due to a decline in perovskite top cell shunt resistance (RSh), has the most severe impact on the EY, emphasizing the imperative to rectify perovskite imperfections in thin film processing causing RSh decline. Second, we investigate implications of degradation in the perovskite top cell on the EY of current mismatched tandem solar cells. Third, we examine critical thresholds for the "acceptable degradation levels" in the perovskite top cell with regard to degradation in each solar cell parameter, assuming that the total loss in EY must be comparable to the degradation in state-of-the-art silicon. Overall, our study highlights that degradation of the perovskite top cell needs to be assessed with care when extrapolating the impact on the lifetime EY of perovskite-silicon tandem solar cells. The severity of degradation for different degradation mechanisms in a single junction perovskite solar cell cannot be translated one-to-one to tandem devices.

1. Introduction

Tandem solar cells bear the potential to overcome the practical power conversion efficiency (PCE) limit of crystalline silicon (c-Si) single-junction (SJ) solar cells around 29%.[1] Perovskite semiconductors are excellent candidates for top cells in combination with c-Si in tandem solar cells due to their outstanding optoelectronic properties, tunable bandgap, and inexpensive fabrication process.[2–11] Perovskite–silicon tandem photovoltaics (PV) have gained attention by their remarkable efficiency improvements in past years and their potential for even higher efficiency.[12] Combining perovskite and silicon is suitable due to their complementary properties: the well-known durability of silicon solar cells and the optoelectronic properties of perovskite solar cells ensure consistent performance. However, the integration of perovskite materials with silicon PV introduces new challenges, particularly concerning the long-term stability of the perovskite solar cells. Silicon solar cells have undergone extensive development and optimization over the past decades, resulting in highly stable and efficient solar cells in the market. In contrast, due to yet limited durability of perovskite PV,[13–20] their economic breakthrough is only expected several years from now. Although significant efforts have been made to improve the stability of perovskites, the highest durability of perovskite solar cells yet lags the durability of silicon solar modules on the market by around one to two orders of magnitude.[21,22]

The most critical stress factors for degradation in perovskite solar cells are light, temperature, oxygen, moisture, and voltage.[23–27] While advanced encapsulation concepts omit the degradation due to oxygen and moisture ingress, the intrinsic stress of perovskite solar cells under operation due to light, temperature, and voltage yet cannot be omitted.[28] More understanding of perovskite degradation mechanisms is required to identify suitable methods to counteract these degradation mechanisms and improve stability.[29,30]

To date, research on perovskite solar cell stability mostly focuses on degradation effects determined and characterized under standard test conditions (STC).[31,32] While these analyses provide a very valuable understanding of fundamental degradation mechanisms and highlight the relevance of perovskite thin film morphology, composition, or additives for enhanced durability, the long-term stability of a tandem solar cell needs to be quantified considering real-world conditions. However, to date, real-world variations in irradiation spectra, temperature profiles, and angle of incidence are mostly disregarded when assessing and predicting degradation in perovskite–silicon tandem solar cells. Moreover, key performance metrics like the levelized cost of electricity or the energy payback time require reliable modeling of the lifetime energy yield (EY) of perovskite–silicon tandem solar cells factoring in degradation.[33–35]

S. Orooji, U. W. Paetzold
Institute of Microstructure Technology
Karlsruhe Institute of Technology, Hermann-von-Helmholtz-Platz 1
76344 Eggenstein-Leopoldshafen, Germany
E-mail: ulrich.paetzold@kit.edu

S. Orooji, U. W. Paetzold
Light Technology Institute
Karlsruhe Institute of Technology
76131 Engesserstrasse 13, Karlsruhe, Germany

The ORCID identification number(s) for the author(s) of this article can be found under https://doi.org/10.1002/ente.202400998.

**ADVANCED
SCIENCE NEWS**

www.advancedsciencenews.com

Energy Technology

Generation, Conversion, Storage, Distribution

www.entechnol.de

This study investigates the EY of perovskite–silicon tandem solar cell undergoing degradation in the perovskite top cell using an advanced EY modeling software named EYCalc.[36] While a recent study[37] has also examined degradation in the context of EY, this article takes a different approach to study degradation. In this study, we aim to determine how degradation in individual solar cell parameters (i.e., open-circuit voltage (V_{OC}), short-circuit current density (J_{SC}), and fill factor (FF)) affect the EY of perovskite–silicon tandem solar cell.

In the first section, we recapitulate the effect of degradation in the individual solar cell parameter of the perovskite and silicon subcells on the solar cell performance under STC. In the second section, we build the analysis of the EY on the understanding of impact of the degradation of individual solar cell parameters on the perovskite/silicon tandem solar cell but consider realistic irradiation conditions. First, we compare the EY of perovskite–silicon tandem solar cell that exhibits degradation in individual solar cell parameters. Our analysis reveals that degradation of individual solar cell parameters results in diverse performance loss characteristics of tandem solar cells. We study degradation in individual solar cell parameters but at the level of diode parameters, i.e., the dark saturation current density (J_0), the collection efficiency (CE), the series resistance (R_S), or the shunt resistance (R_{Sh}). Although real degradation mechanisms affect multiple parameters simultaneously, we analyze the effect of each diode parameter on the tandem solar cell EY separately. This is because the simultaneous change of multiple parameters makes it difficult to understand the specific impact of each individual diode parameter. To ensure the robustness of our results, we evaluate the EY of tandem solar cells across various climate zones (i.e., Phoenix (arid/desert), Seattle (temperate), and Honolulu (tropical/humid areas), see Figure SI 1 and SI 2). Next, we explore the effects of perovskite top cell degradation on the EY of mismatched tandem solar cells. This analysis aims to determine which current-mismatch scenario provides the highest EY over the entire lifetime (i.e., 30 years). This approach helps to optimize the balance between the current of perovskite top cell and the silicon bottom cell, allowing for an understanding of which device architecture (current-matching scenario) is optimum based on the total lifetime EY considering degradation. Finally, we examine critical thresholds for the "acceptable levels of degradation" in the perovskite top cell regarding degradation in each solar cell parameter. Our analysis aims to determine the maximum acceptable degradation such that the total EY loss over the entire lifetime of the tandem solar cell remains comparable to the degradation levels observed in state-of-the-art silicon PV (i.e., a maximum of 0.5% per year).

This study is implemented at the level of diode parameters due to the lack of clarity regarding the impact of real degradation mechanisms on diode parameters. Once a definitive interrelation between degradation mechanisms and variations in diode parameters has been established by the field, our EY modeling framework (EYCalc) will be capable of making predictions concerning specific degradation mechanisms. This study is intended to be universally applicable to all types of perovskite solar cells. Therefore, specific material characteristics are not considered, and our focus is solely on the bandgap of the materials.

2. Experimental Section

This study computes the EY of perovskite–silicon tandem solar cells factoring in degradation using our in-house developed EY modeling platform, EYCalc. The software is published as an open-source software project.[34] A comprehensive description of the software is provided by Schmager et al.[34] It consists of four modules: the irradiance module, the optics module, the electrical module, and the EY module. The irradiance module computes, based on data from the typical meteorological year (TMY3)[38] for various locations in the USA, the direct and diffuse irradiance spectra for each hour of the year. It feeds the meteorological data of the TMY3 dataset into the simplified model of atmospheric radiative transfer of sunshine[39] to compute the clear sky irradiance. Further, a basic cloud model is used to account for the weather. The optics module employs the transfer-matrix method to evaluate thin layers that are optically coherent and utilizes a series expansion based on the Beer–Lambert law for the analysis of thick layers that are optically incoherent. This approach allows for the calculation of reflectance, transmittance, and absorptance that are resolved both spectrally and angularly for each layer within the stack. Additionally, the optics module is capable of simulating stacks that include textured interfaces through the use of geometrical ray-tracing, as documented by Baker–Finch and McIntosh.[40]

The electrical module determines the temperature-dependent current density–voltage (J–V) characteristics of the perovskite–silicon tandem solar cell. In this study, we expanded the electrical module to account for degradation in the solar cell parameters V_{OC}, J_{SC}, and FF of the perovskite–silicon tandem solar cell. The degradation is implemented at the level of the diode parameters (i.e., the dark saturation current density (J_0), the CE, the series resistance (R_S), or the shunt resistance (R_{Sh})), which relate back to the solar cell parameters (see **Figure 1**). The numerical calculations are performed by a coupled two-diode model in LTspice.[41] Finally, the core EY module calculates the EY of perovskite–silicon tandem solar cells over the entire lifetime considering the solar module orientation (rotation and/or tilt of the module) and location. Thereby, we calculate the EY of perovskite–silicon tandem solar cells for up to 30 years, factoring in different degradation scenarios to assess the long-term impact on the EY. We examined the aggregated EY over 30 years across different climatic locations to further assess the degradation effects. Temperature effects are intrinsically considered, using the nominal operating cell temperature (NOCT) model.[42] In our model, we assumed a NOCT of 48 °C and extracted the insolation on the cell and ambient air temperature from TMY3 data. The architecture of the reference cell used in this study, as well as the corresponding experimental and simulated electrical and optical values are shown in Figure SI 3.

3. Results and Discussions

This study analyzes the EY of perovskite–silicon tandem solar cells undergoing degradation in the perovskite top cell. This study aims to reveal the extent to which degradation in the solar cell parameters (V_{OC}, J_{SC}, and FF) impacts the overall EY. Currently, there is no clear understanding of how the real
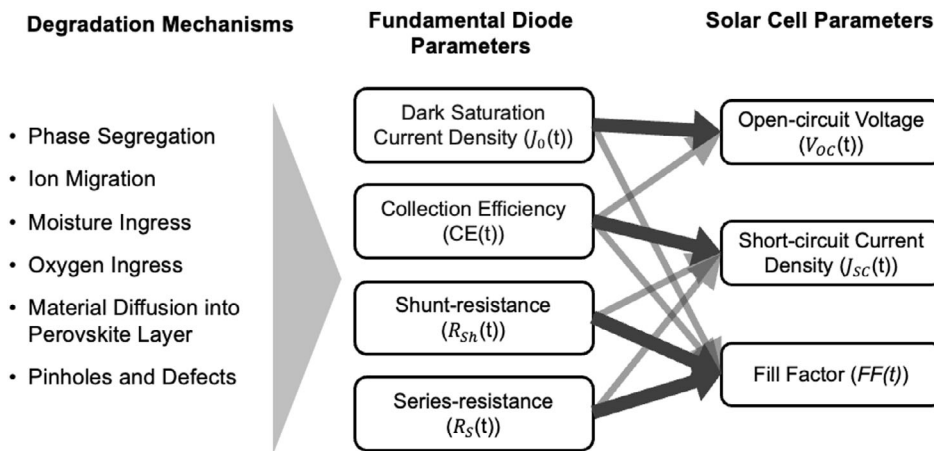
Figure 1. Relationship between solar diode parameters and solar cell parameters, including the widely recognized degradation mechanisms. Thick gray arrows indicate significant impact, while the thin gray arrows highlight less prominent effects.

degradation mechanisms affect the diode parameters (i.e., J_0, CE, R_S, and R_{Sh}). Therefore, we implement this study at the level of diode parameters. Once the field establishes clear interrelation of specific degradation mechanism and the variation in diode parameters, our EY framework (EYCalc) will be able to perform this study and make predictions with regard to the specific degradation mechanisms. However, this study establishes a foundation for the future studies in the field of degradation with regard to the EY.

Figure 1 illustrates the correlation between the diode parameters and the solar cell parameters to identify how specific changes in diode parameters affect key solar cell parameters. While the exact interdependences between these parameters are complex, we can observe specific trends: the decrease in J_0 predominantly affects the V_{OC}, the CE impacts mostly the J_{SC}, and degradation in FF is at foremost attributed to an increment in R_S and decline in R_{sh} (see Figure 1). In the following, we revisit the interrelation of prominent degradation mechanisms described in the literature and degradation in solar cell parameters. a) *Degradation of current generation in the perovskite top cell:* Degradation of current generation in perovskite solar cells is effectively described by a reduction in CE that linearly correlates to the J_{SC}. A prominent degradation mechanism attributed to a reduction in CE is halide phase segregation. Halide phase segregation forms localized domains with higher concentration of halide ions, leading to trapping the charge carriers and a decrease in CE.[43–45] b) *Degradation of FF in the perovskite top cell:* Degradation of FF in perovskite solar cells is well described by a reduction in R_{Sh} or an increment in R_S. A decrease in R_{Sh} is a common problem in imperfect perovskite solar cells that can be associated, for example, with the presence of pin holes or defects in the thin film morphology that result in shunts between the top and rear electrode. Other examples of mechanisms resulting in a decrease in R_{Sh} are 1) the diffusion of hole transport layer dopants into the perovskite layer or 2) interdiffusion of metal and halide ions between the perovskite layer and the metal contact.[46–48] A prominent degradation mechanism associated with increment in R_S is ion migration. Due to the accumulation

of halide ions in the vicinity of the charge transport layers, ion migration induces an effective barrier for the charge extraction and leads to a higher R_S.[49] Another example of increased R_S is the degradation of transparent and conducting electrodes.[50] c) *Degradation in voltage of the perovskite top cell:* Degradation of V_{OC} in perovskite solar cells is perfectly described by an increase in J_0. Nonradiative charge carrier recombination at the surface, in the bulk, and at grain boundaries results in a high leakage current from grain boundaries, which raises J_0.

In the first part of our study, we revisit the effect of degradation of individual solar cell parameters in perovskite top and silicon bottom cells (i.e., V_{OC}, J_{SC}, and FF) on the performance of tandem solar cell under STC. In the second next section, we project the EY of perovskite–silicon tandem solar cells undergoing various degradation scenarios. A schematic overview of the EY modeling factoring in degradation is shown in **Figure 2**. We highlight that the degradation is discussed with regard to solar cell parameters (i.e., V_{OC}, J_{SC}, and FF), but implement the degradation at the level of the diode parameters, i.e., J_0, CE, R_S, and R_{Sh}. It should be noted that when analyzing the impact of degradation on a specific solar cell parameter due to a variation in the interrelated diode parameter, the remaining diode parameters remain unchanged. For instance, when analyzing J_{SC} degradation through a decline in CE, the other diode parameters (J_0, R_S, and R_{Sh}) remain constant. By analyzing the effect of each parameter separately, we can better understand how changes in individual diode parameters affect the lifetime EY of perovskite/silicon tandem solar cells that undergo degradation. Although real degradation mechanisms affect many parameters at once, our method helps to see the specific impacts of each individual parameter on the overall EY. This approach prevents confusion that could arise from changing multiple parameters at the same time, which can hide the true relationships.

3.1. Performance Under STC Factoring in Degradation

In this section, we examine how degradation effects the performance of perovskite–silicon tandem solar cell under STC. The
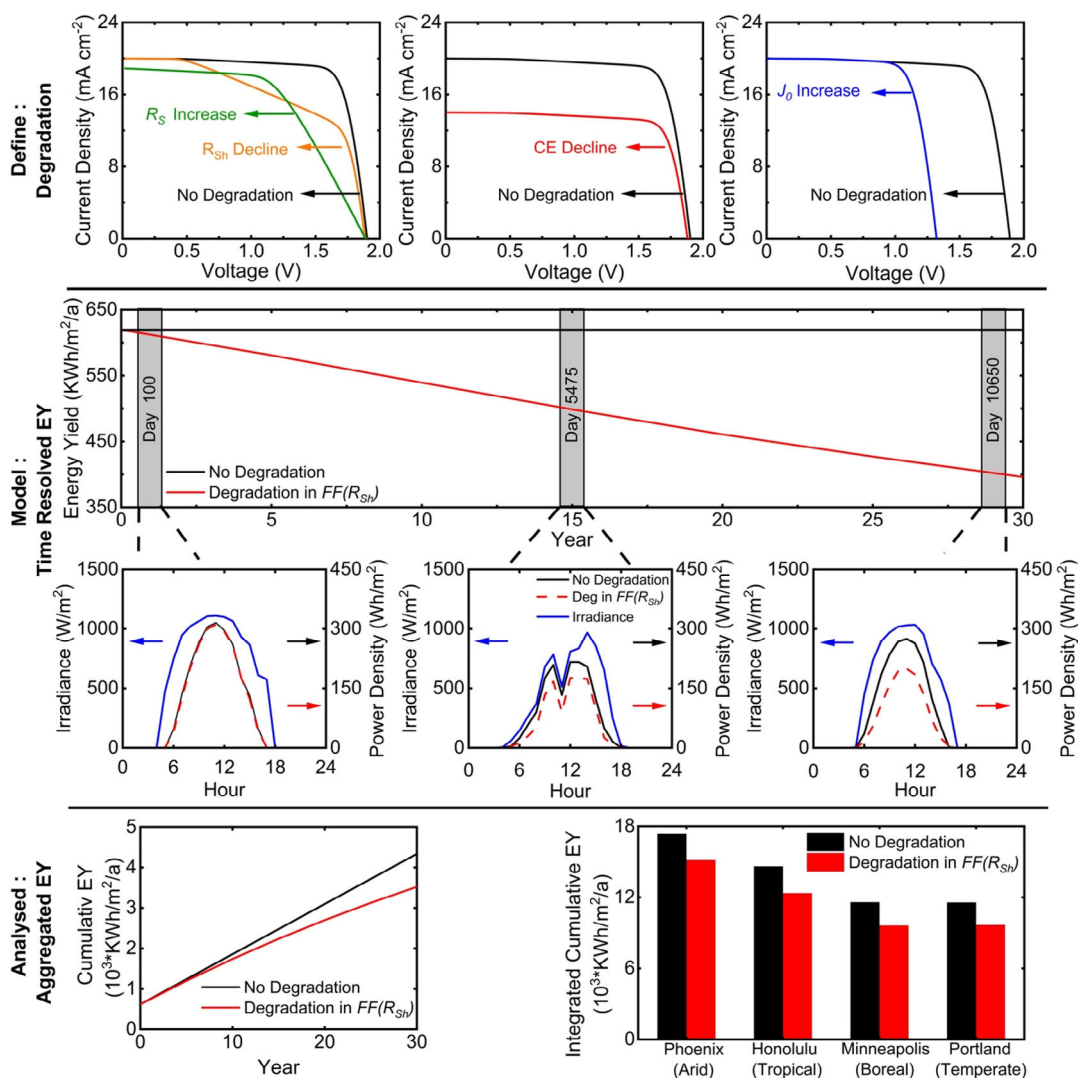
ADVANCED
SCIENCE NEWS
www.advancedsciencenews.com

Energy Technology
Generation, Conversion, Storage, Distribution

www.entechnol.de

Figure 2. The methodology used for this study, including 1) type of degradation, 2) modeling time-resolved EY for every hour of the 30 year lifetime, and 3) analyzing the effect of degradation on tandem solar cell EY by computing aggregated EY over 30 years in different climatic conditions.

degradation is discussed for the individual solar cell parameters (V_{OC}, J_{SC}, and FF) and implemented at the level of the diode parameters. We recapitulate that degradation in individual solar cell parameters has diverse effects on tandem solar cell performance. a) First, we investigate the degradation in V_{OC} due to an increment in J_0 for each subcell. We reiterate that the superposition of V_{OC} in the subcells is maintained for tandem solar cells regardless of variations in J_0 in the subcells (see Figure SI 4). This superposition also holds true for the tandem solar cell efficiency (see **Figure 3**). Furthermore, we demonstrate that the overall effect of variation in subcells J_0 on tandem solar cell V_{OC} scales with the relative contribution to the V_{OC} of the subcells ($\approx 14\%$ and $\approx 8\%$ drop in V_{OC} of the tandem solar cell for a 20% degradation in the V_{OC} of the perovskite top and silicon bottom cells, respectively (see Figure SI 4)). b) Second, we discuss the performance of tandem solar cell undergoing degradation in FF (due to an increment in R_S or decline in R_{Sh}) in the perovskite

top cell. Our findings reveal a pronounced superlinear degradation in FF and PCE of the tandem solar cell for decreased R_{Sh} (see **Figure 4**). Conversely, increment in R_S of the perovskite top cell shows a linear relationship with the FF and PCE of the tandem solar cells (see Figure SI 4).

However, we note that the correlation shown in Figure 4 is more complex for mismatched perovskite/Si tandem solar cells. As reported in the literature,[51] FF increases for slightly mismatched tandem solar cells. The extent of this effect correlates with the R_{Sh} of the current-limiting subcell. Reduced R_{Sh} of either subcells provides an alternative current path for matching the top and bottom cell currents, which affects the overall tandem solar cell J_{SC} and FF. In **Figure 5**, we discuss the impact of current mismatch on tandem solar cell FF. We indicate our result for different levels of current mismatch (± 4 mA cm^{-2}) and different values for the R_{Sh} of the perovskite top cell. Our results reveal that the FF of the tandem solar cell increases as the R_{Sh} in
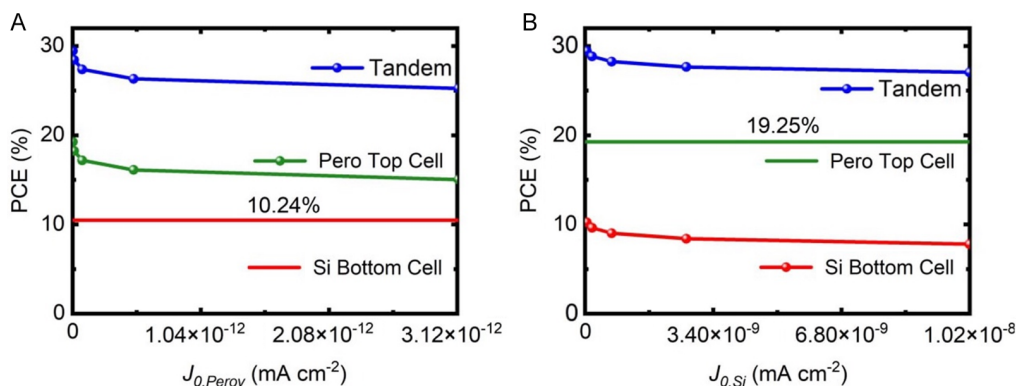
Figure 3. Variation in J_0 of subcells and consequent degradation in tandem solar cell and A) perovskite top cell and B) silicon bottom cell PCE.
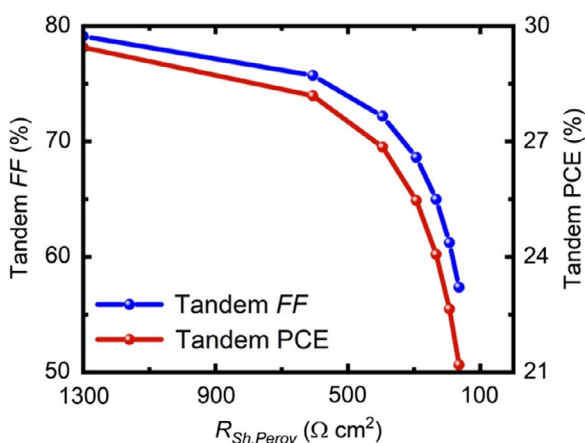

Figure 4. Decline in R_{Sh} of the perovskite top cell and resulting FF and PCE of the respective perovskite/Si tandem solar cell.
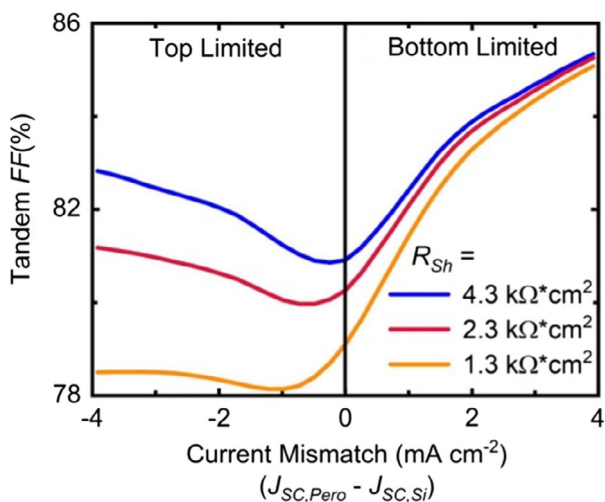

Figure 5. FF of perovskite/Si tandem solar cell as a function of current mismatch for different values of the R_{Sh} in the perovskite top solar cell.

the perovskite top cell increases. Moreover, the overall increase in the FF caused by current mismatch is more pronounced for tandem solar cells limited by current generation in the bottom sub

cell. This is because the R_{Sh} of the silicon bottom cell is much larger compared to the perovskite top cell. The discussion highlights that reducing current mismatch in a top-limited tandem solar cell does not necessarily lead to a decrease in FF. If the R_{Sh} of the perovskite top cell is relatively low, FF may increase instead of an expected decrease (see Figure 5, compare $R_{Sh} = 1.3\,k\Omega\,cm^2$ and $R_{Sh} = 4.3\,k\Omega\,cm^2$). Furthermore, it is important to note that given a relatively low R_{Sh} of the perovskite top cell, the FF of the perovskite-limited tandem solar cell is even lower than that of the current-matched cell. c) Third, we discuss the performance of tandem solar cell undergoing J_{SC} degradation (due to a decline in CE) in the perovskite top and the silicon bottom cells. As shown in **Figure 6**, the PCE of the tandem solar cell does not decrease linearly with decreasing CE of perovskite top and silicon bottom cells. While a reduction in CE results in an expected linear decrement in tandem solar cell J_{SC} of the respective subsolar cell, the overall impact on PCE is much more complex. The monolithic interconnection implies that the impact on the PCE highly depends on whether the tandem solar cell is limited by the perovskite top cell, or the Si bottom cell (see Figure 6). Tandem solar cells with limited current generation in the top cell experience a significantly enhanced degradation in J_{SC} compared to current-matched or bottom-limited tandem cells if the CE of the perovskite top cell decreases. While there is a slight increment in FF for the top-limited cells due to low R_{Sh} (compared to a decrease for other current-matching conditions), the degradation in J_{SC} outweighs the mild increase in FF. Overall, the top-limited cell experiences more substantial decline in PCE with respect to other current-matching scenarios (see Figure 6A).

On the other hand, if the CE of the silicon bottom cell is reduced instead, a similar overall effect in J_{SC} is observed, indicating that bottom-limited devices are more vulnerable to changes in J_{SC}. However, the overall impact is substantially different because FF improves for all current-matching conditions. This results in a reduced decline in normalized PCE compared to corresponding perovskite top cell cases (see Figure 6B).

3.2. EY Modeling and Degradation

Here, we investigate the EY of perovskite–silicon tandem solar cells factoring in degradation in different solar cell parameters of the perovskite top solar cell. The focus is set on the implication
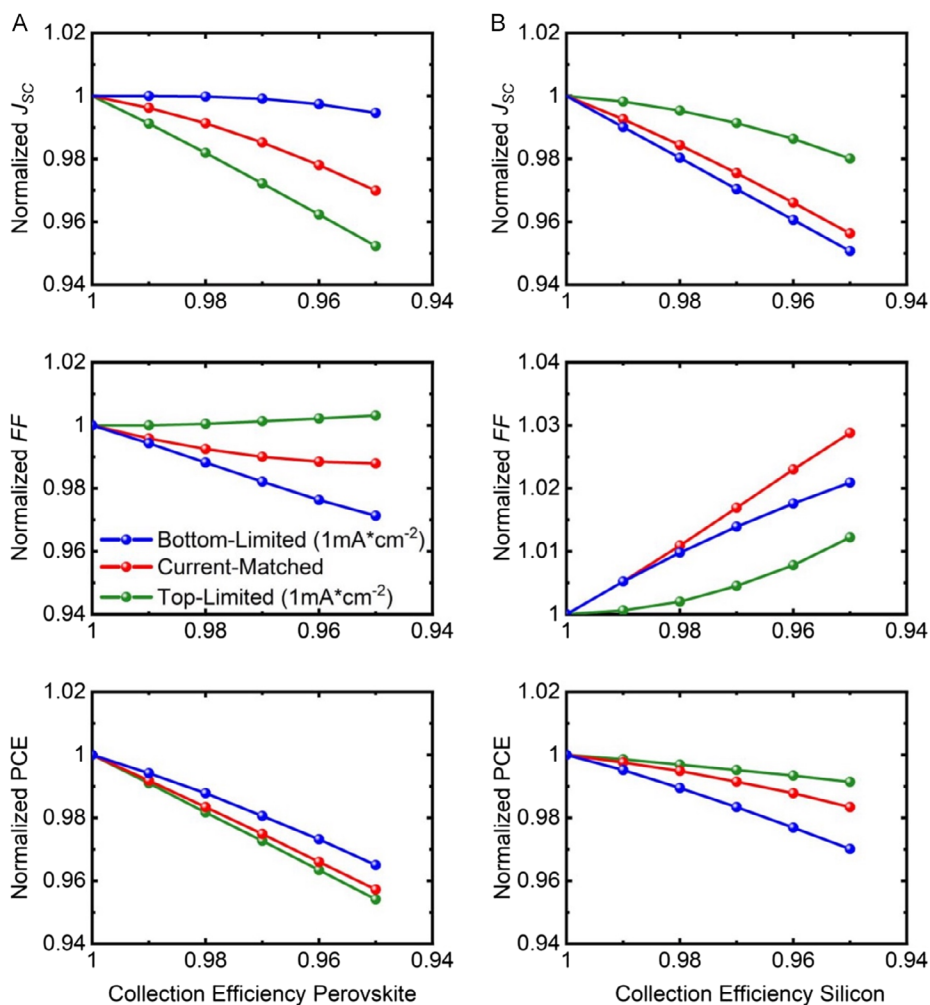
Figure 6. Impact of 5% decline in CE of the perovskite top solar cell A) and silicon bottom solar cell B) on the solar cell parameters (J_{SC}, FF, and PCE) of the perovskite–silicon tandem solar cell. Different scenarios of current matching are considered. To facilitate the comparison, we compare the normalized solar cell parameters.

of degradation on the EY of various tandem solar cell architectures. As highlighted in the previous section, degradation of SJ solar cell parameters of perovskite top solar cell cannot be translated one-to-one to tandem devices. Moreover, degradation in EY of tandem solar cells varies between locations, due to the interdependencies of the individual solar cell parameters and environmental factors such as irradiation intensity and spectrum. To shed light on these interdependencies, we focus on three distinct geographical locations (see Figure SI 1 and SI 2): Phoenix (arid/desert location), Seattle (temperate location), and Honolulu (tropical/humid).

3.2.1. EY of Tandem Solar Cells with Degradation across Various Locations

First, we assess the EY of tandem solar cells undergoing uniform degradation of 10% in individual perovskite top cell solar cell parameters. The EY is evaluated for various locations. This study

enables us to determine the one solar cell parameter whose degradation has the highest impact on tandem solar cell EY. Our analysis reveals that a 10% degradation in the FF of the perovskite top cell due to a decline in R_{Sh} and an increment in R_S, respectively, shows the highest and lowest impact on tandem solar cell EY regardless of location (see **Figure 7** and Figure SI 5). This result emphasizes the importance of rectifying perovskite imperfections in thin film processing causing R_{Sh} decline. In real-world conditions, there is an interdependency between degradation mechanisms and their effects on diode parameters, as well as between the variations in one diode parameter and others. However, isolating and assessing the impact of each diode parameter separately is insightful to understand how variation in individual diode parameter affects the overall EY.

The observations are consistent with the analysis of degradation under STC, i.e., the observed superlinear relationship between the performance of the tandem solar cell and the decline in R_{Sh} of the perovskite top cell (see Figure 4 and 5). Furthermore, the minimal impact of an increase in R_S on
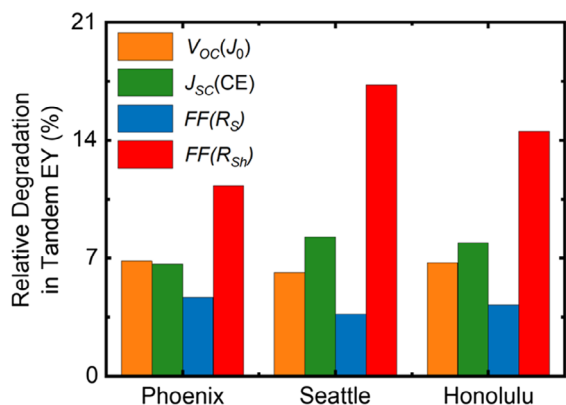
Figure 7. Relative degradation in tandem solar cell EY undergoing 10% degradation of the V_{OC}, J_{SC}, and FF implemented by variation in the diode parameters (J_0, CE, R_S, and R_{Sh}) of the perovskite top cell in Phoenix, Seattle, and Honolulu.

tandem solar cell EY aligns with the linear relationship between tandem solar cell performance and R_S increment (see Figure SI 5). This effect also aligns with its relatively minor impact on other solar cell parameters, such as V_{OC} and J_{SC}. Moreover, the variation in the impact of degradation in J_{SC} and V_{OC} of the perovskite top cell on the tandem solar cell EY in different locations was anticipated due to the established proportional relationship between J_{SC}, V_{OC}, and light intensity.[52]

3.2.2. EY of Current-Mismatched Tandem Solar Cells with Degradation

Next, we investigate the EY of tandem solar cells with different current-matching conditions undergoing degradation. This study aims to reveal how different current-matching conditions of our tandem solar cell under STC affect the lifetime EY considering degradation. It is crucial to highlight that the different current-matching configurations examined in this study refer to cells that are initially mismatched under STC. Subsequently, their performance is evaluated under realistic irradiation conditions.

To provide different levels of current mismatch over time, we incorporate two distinct levels of CE decline rates (1% and 2% annually). We compare the lifetime EY of a tandem solar cell installed in Phoenix (see **Figure 8**A,B) which exhibit three levels of initial current mismatch. The current mismatch is determined under STC.

The top-limited tandem solar cell with a 10% current mismatch ($\approx 2\,\text{mA}\,\text{cm}^{-2}$) experiences the most significant reduction in EY due to linear degradation in J_{SC} of the tandem solar cell. In contrast, the bottom-limited counterpart exhibits the lowest decline (see Figure 8A,B). In the first 12–15 years, the current-matched tandem solar cell shows the highest EY, while the bottom-limited counterpart shows the lowest EY. However, in the second half of the lifetime, the EY of the current-matched tandem device is much lower compared to the EY of the bottom-limited solar cells. For a more detailed dataset
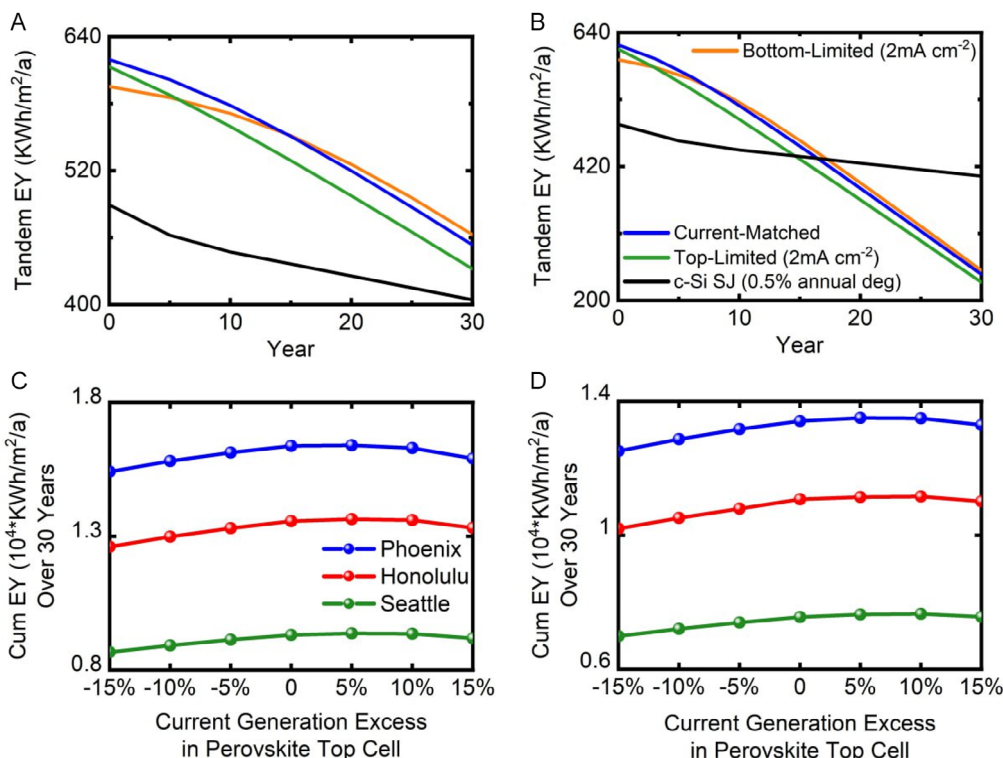

Figure 8. EY of perovskite–silicon tandem solar cell as well as c-Si SJ solar cell[55] located in Phoenix undergoing a current generation decline in the perovskite top cell: A) 1% annual decline in CE and B) 2% annual decline in CE. Lifetime EY (30 years) for different levels of initial current mismatch of the perovskite-silicon tandem solar cell in Phoenix, Seattle, and Honolulu factoring in J_{SC} degradation with annual CE decline rate of C) 1% and D) 2%.

**ADVANCED
SCIENCE NEWS**

www.advancedsciencenews.com

Energy Technology
Generation, Conversion, Storage, Distribution

www.entechnol.de

encompassing more increments in current mismatch of the tandem solar cell and various locations, we refer to Figure SI 7. Over the entire lifetime, bottom-limited tandem solar cell with ≈5% current mismatch, undergoing J_{SC} degradation, exhibits the highest cumulative EY over 30 years. It is highlighted that this cumulative EY is even higher than that for an optimum tandem solar cell architecture, i.e., a current-matched tandem solar cell (see Figure 8C,D). The findings are consistent across different locations (see Figure SI 7). In summary, this study shows that a moderate initial current limitation of the bottom solar cell by around 5–10% is optimal for a 30 year lifetime if the top solar cell undergoes J_{SC} degradation (≈1% and ≈2% annual). Furthermore, considering degradation in current generation of the top solar cell results in a rather broad optimal device architecture with regard to the current matching, if the device is initially moderately bottom limited.

3.2.3. Comparing Degradation in EY and STCs

Next, we indicate the difference between degradation impact on the tandem solar cell performance under STC and its EY. We also investigate the tandem solar cell EY undergoing degradation in different solar cell parameters at different rates. We examine the EY in two scenarios: (1) matching the degradation rate of the perovskite top cell to that of state-of-the-art c-Si solar cells (0.5% per year[53]) and (2) a significantly higher degradation rate of 2% per year.

To discriminate the effect of degradation in different solar cell parameters on the EY and its efficiency, we compare the scenarios where degradation rates of 0.5% and 2% are solely caused by degradation in V_{OC}, J_{SC}, or FF. For rather low degradation rates of 0.5%, similar to previous analyses (see Figure 7), we find that the EY of the tandem solar cell decreases linearly but at different rates for each degradation scenario. The tandem solar cell EY exhibits fastest degradation for a decline in the perovskite top cell's R_{Sh}. Conversely, the impact of FF degradation caused by an increment in perovskite top cell's R_S is the lowest (see **Figure 9**A). Interestingly, for degradation rates exceeding the degradation of state-of-the-art silicon PV (e.g., 2%), the degradation in FF due to a decline in R_{Sh} shows an asymptotic behavior (see Figure 9B). For low R_{Sh} in the perovskite top solar cell, the tandem solar cell is effectively shunted, and the EY of the tandem solar cell approaches the EY of the silicon bottom cell only. Thus, the asymptotic behavior must not be confused with stabilization or a deceleration in degradation.

Furthermore, we compare the degradation in EY to the degradation in PCE (see Figure 9C). The direct comparison of the lifetime EY and lifetime degradation in PCE of tandem solar cells (see Figure 9C) highlights that the performance under STC does
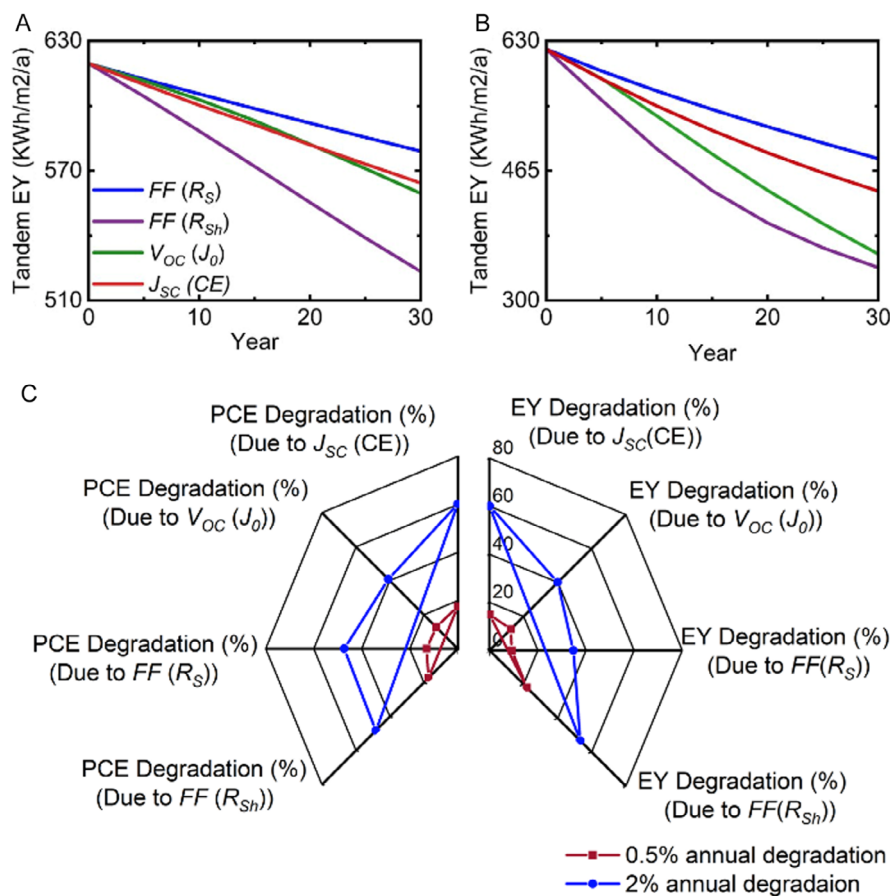

Figure 9. Tandem solar cell EY undergoing degradation with absolute annual degradation of A) 0.5% and B) 2% in perovskite top cell in Phoenix. C) Comparison between the effect of 0.5% and 2% absolute annual degradation in perovskite top cell on tandem solar cell PCE and EY (Phoenix).

not accurately reflect realistic irradiation conditions. For example, considering a 2% degradation per year in the FF of the perovskite top solar cell due to an increment in R_S, the extrapolation performance degradation of PCE predicts a loss of almost 32%, while the actual loss in lifetime EY due to degradation is only around 22%. The reason for this enormous discrepancy is the wide variation in solar intensity that is considered in EY calculations which consider real-world irradiation scenarios but disregarded in the assessment of the PCE determine under STC. Similar but less severe differences in lifetime PCE and lifetime EY are apparent for the FF degradation due to decline in R_{Sh}.

3.2.4. Permissible Level of Degradation in Top Cell Solar Cell Parameters

Next, we examine critical thresholds for the "acceptable levels of degradation" in the perovskite top solar cell with regard to degradation in each solar cell parameter, assuming that the total loss in EY over the lifetime of a perovskite tandem must be comparable to the degradation in state-of-the-art silicon PV ($\approx$0.5% in performance[53]). For comparison, to date, one of the lowest reported degradation rates of perovskite PV is in the range of 1.4% in only 1000 h.[54] This discrepancy highlights the tremendous efforts that are required in the upcoming years to improve the durability of perovskite PV. However, to date, it is not even clear what is the sufficient stability, i.e., the "acceptable level of degradation", for the perovskite top solar cell, considering that the degradation in the top solar cells does not linearly impact the EY of the tandem solar cell.

In response, we flip the perspective in this last section and determine backward the acceptable level of degradation in a single solar cell parameter of the perovskite top solar cell assuming a maximum overall degradation of 0.5% per year in the tandem solar cell. To discriminate the effect of degradation in different solar cell parameters, we compare the scenarios where degradation is solely caused by degradation in V_{OC}, J_{SC}, or FF (see

Figure 10). Our results show that if the stated loss is attributed solely to degradation in V_{OC} (resulting from an increase in J_0), there is overall a rather low level of V_{OC} degradation at the end of the lifetime of up to $\approx$18% which can vary depending on climate zone. This degradation in V_{OC} corresponds to $\approx$3000-fold increase in J_0, which is significant as it leads to higher leakage current and increased degradation over time. Conversely, if the mentioned loss is due to J_{SC} degradation (resulting from a decline in CE), the acceptable J_{SC} degradation exceeds 15%, contingent upon the climate zone. This 15% J_{SC} degradation equates to an approximate 18% decline in CE. However, when the specified decline in tandem solar cell EY results from FF degradation, the acceptable level of FF degradation varies depending on whether it arises from a decrease in R_{Sh} or an increase in R_S.

In summary, our study reveals that the permissible degradation level in the perovskite top cell varies depending on climate zone and the solar cell parameter responsible for the degradation.

4. Conclusion

Perovskite/Si tandem PV has emerged as a promising technology due to its potential for high efficiency and low-cost production. However, integrating perovskite materials with silicon presents new challenges concerning the yet limited durability of the perovskite material. While previous research on the stability of perovskite provides valuable understanding in this topic, studying degradation in real-world conditions is often disregarded. This study shows how degradation in individual solar cell parameters (i.e., V_{OC}, J_{SC}, and FF) of the perovskite top cell affects the EY of perovskite–silicon tandem solar cell. We assess long-term tandem solar cell EY undergoing different degradation scenarios. First, we assess tandem solar cell EY undergoing degradation of individual solar cell parameter (V_{OC}, J_{SC}, and FF) in the perovskite top cell. However, as to date there is no clear understanding of how degradation mechanisms interrelate with
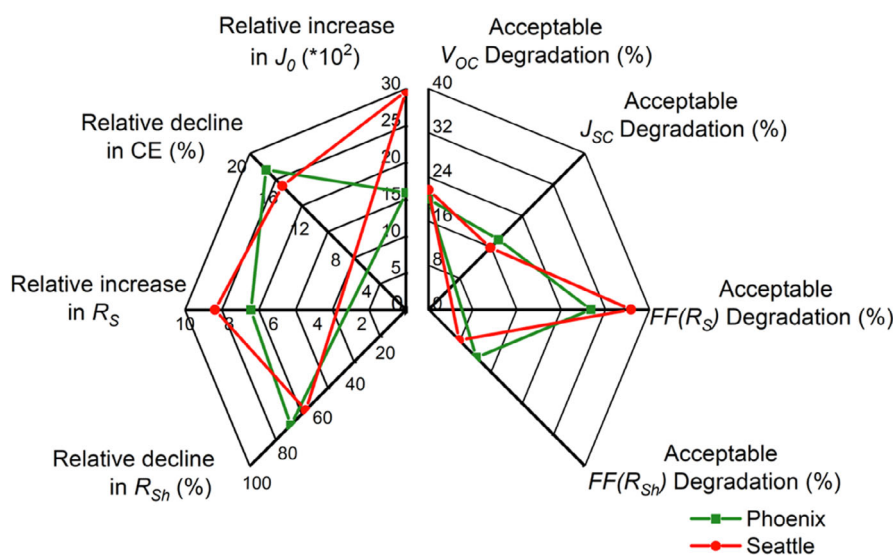

Figure 10. Permissible levels of degradation in V_{OC}, J_{SC}, and FF and corresponding variation in the contributing diode parameters, i.e., CE, J_0, R_S, and R_{Sh}, respectively, for 0.5% annual degradation in tandem solar cell EY over 30 years in different climatic conditions.

the diode parameters, we perform our study at the level of diode parameters (i.e., J_0, CE, R_S, and R_{Sh}). This analysis provides the foundation for the future studies. Once a definitive interrelation between real degradation mechanisms and variation in diode parameters identified, our EY modeling framework will be able to perform analysis in the context of specific degradation mechanisms.

Our results demonstrate that degradation in FF of perovskite top cell due to a decline in R_{Sh} and an increment in R_S has the most and least significant effect on tandem solar cell EY, respectively. This shows the importance of rectifying perovskite imperfections in thin film processing as the leading cause of R_{Sh} decline. Furthermore, our analysis reveals that the influence of degradation on tandem solar cell EY varies across different climatic zones, providing region-specific insights for optimization.

Next, we demonstrate the EY of mismatched tandem solar cells undergoing degradation. We focus on J_{SC} degradation in this analysis, as it modifies the current mismatch over time and effectively represents the interplay between mismatched tandem solar cell EY and degradation. Based on our research, a slightly bottom-limited cell, undergoing J_{SC} degradation, has the highest cum EY over 30 years across various climate zones. Furthermore, we illustrate that keeping the initial current mismatch of a bottom-limited cell, undergoing J_{SC} degradation, within a 10% margin results in minimal EY loss. Understanding the precise value (referring to a 5% bottom-limited scenario) and margin (5–10%) for bottom limitations despite degradation ensures minimal EY loss of tandem solar cells, which is crucial for industrial implementation. This analysis helps manufacturers optimize device architecture for maximum lifetime EY, enhance durability by selecting materials and designs suited for various climate zones, and maintain performance stability by controlling initial current mismatch.

Next, we assess long-term tandem solar cell EY when the perovskite top cell undergoes degradation rates equal to or higher than the observed degradation rate in c-Si solar cells (0.5% and 2% annually, respectively). Our analysis reveals a potential exclusion of the perovskite top cell from the tandem solar cell when the degradation rate of the perovskite top cell surpasses a certain threshold (>2% annually).

Finally, we examine critical thresholds for the "acceptable levels of degradation" in the perovskite top solar cell with regard to degradation in each solar cell parameter. This analysis is done by assuming that the total EY loss over the lifetime of a perovskite-silicon tandem must be comparable to the degradation in c-Si solar cells (i.e., max. 0.5% per year). This analysis provides a comprehensive understanding of EY degradation in perovskite–silicon tandem solar cells and the overall impact of degradation in the individual solar cell parameters. This analysis aids manufacturers in designing solar cells suitable for different climate zones by considering the impact of environmental factors such as light intensity, humidity, and temperature on diode parameters. Understanding the acceptable degradation rate in each parameter provides target values for optimizing the materials used in solar cells ensuring enhanced durability and performance.

In future research, we foresee to compare the experimental stability data of perovskite–silicon tandem solar cells with the simulated EY data. This comparison will be instrumental while designing experiments replicating the simulation conditions and providing a robust benchmark, enabling a deeper understanding of degradation mechanisms and their impact on EY. While the experimental datasets on EY of perovskite/silicon tandem PV are limited today, we expect that the number of such datasets will strongly increase in the near future, given rise to many research questions that can be addressed with our EY framework (EYCalc). We believe that an industrial implementation to the analyses conducted in this study, such as the analysis of initially mismatched tandem solar cells, with the objective of identifying the optimal device architecture (current-matching scenario) based on total lifetime EY, represents a fruitful avenue for future research.

Supporting Information

Supporting Information is available from the Wiley Online Library or from the author.

Acknowledgements

Conflict of Interest

The authors declare no conflict of interest.

Data Availability Statement

The data that support the findings of this study are available from the corresponding author upon reasonable request.

Keywords

[1] L. C. Andreani, A. Bozzola, P. Kowalczewski, M. Liscidini, L. Redorici, *Adv. Phys. X* **2019**, *4*, 1548305.

[2] D. P. McMeekin, G. Sadoughi, W. Rehman, G. E. Eperon, M. Saliba, M. T. Hörantner, A. Haghighirad, N. Sakai, L. Korte, B. Rech, M. B. Johnston, L. M. Herz, H. J. Snaith, *Science* **2016**, *351*, 151.

[3] E. Aydin, T. G. Allen, M. De Bastiani, L. Xu, J. Ávila, M. Salvador, E. Van Kerschaver, S. De Wolf, *Nat. Energy* **2020**, 5, 851.

[4] L. Wang, Q. Song, F. Pei, Y. Chen, J. Dou, H. Wang, C. Shi, X. Zhang, R. Fan, W. Zhou, Z. Qiu, J. Kang, X. Wang, A. Lambertz, M. Sun, X. Niu, Y. Ma, C. Zhu, H. Zhou, J. Hong, Y. Bai, W. Duan, K. Ding, Q. Chen, *Adv. Mater.* **2022**, 34, 2201315.

[5] H. Zhou, Q. Chen, G. Li, S. Luo, T. Song, H.-S. Duan, Z. Hong, J. You, Y. Liu, Y. Yang, *Science* **2014**, 345, 542.

[6] F. Sahli, J. Werner, B. A. Kamino, M. Bräuninger, R. Monnard, B. Paviet-Salomon, L. Barraud, L. Ding, J. J. Diaz Leon, D. Sacchetto, G. Cattaneo, M. Despeisse, M. Boccard, S. Nicolay, Q. Jeangros, B. Niesen, C. Ballif, *Nat. Mater.* **2018**, 17, 820.

[7] H. Shen, S. T. Omelchenko, D. A. Jacobs, S. Yalamanchili, Y. Wan, D. Yan, P. Phang, T. Duong, Y. Wu, Y. Yin, C. Samundsett, J. Peng, N. Wu, T. P. White, G. G. Andersson, N. S. Lewis, K. R. Catchpole, *Sci. Adv.* **2018**, 4, eaau9711.

[8] D. Kim, H. J. Jung, I. J. Park, B. W. Larson, S. P. Dunfield, C. Xiao, J. Kim, J. Tong, P. Boonmongkolras, S. G. Ji, F. Zhang, S. R. Pae, M. Kim, S. B. Kang, V. Dravid, J. J. Berry, J. Y. Kim, K. Zhu, D. H. Kim, B. Shin, *Science* **2020**, 368, 155.

[9] J. Liu, M. De Bastiani, E. Aydin, G. T. Harrison, Y. Gao, R. R. Pradhan, M. K. Eswaran, M. Mandal, W. Yan, A. Seitkhan, M. Babics, A. S. Subbiah, E. Ugur, F. Xu, L. Xu, M. Wang, A. Rehman, A. Razzaq, J. Kang, R. Azmi, A. A. Said, F. H. Isikgor, T. G. Allen, D. Andrienko, U. Schwingenschlögl, F. Laquai, S. De Wolf, *Science* **2022**, 377, 302.

[10] S. Mondal, M. Chaudhury, P. Chakrabarti, S. Maity, *Energy Fuels* **2023**, 37, 12301.

[11] S. Mondal, A. Jain, S. Maity, *Sol. Energy Mater. Sol. Cells* **2024**, 271, 112869.

[12] National Renewable Energy Laboratory, *Best Research-Cell Efficiency Chart*, https://www.nrel.gov/pv/cell-efficiency.html.

[13] E. Commission, J. R. Centre, A. Jäger-Waldau, *PV Status Report 2018*, Publications Office of the European Union, Luxembourg, **2018**, ISBN 978-92-79-97466-3, https://doi.org/10.2760/924363, JRC113626.

[14] P.-J. Ribeyron, *Nat. Energy* **2017**, 2, 17067.

[15] Y. Li, B. Shi, Q. Xu, L. Yan, N. Ren, Y. Chen, W. Han, Q. Huang, Y. Zhao, X. Zhang, *Adv. Energy Mater.* **2021**, 11, 2102046.

[16] M. A. Green, A. Ho-Baillie, H. J. Snaith, *Nat. Photonics* **2014**, 8, 506-514.

[17] F. Schackmar, H. Eggers, M. Frericks, B. S. Richards, U. Lemmer, G. Hernandez-Sosa, U. W. Paetzold, *Adv. Mater. Technol.* **2021**, 6, 2000271.

[18] J. Roger, L. K. Schorn, M. Heydarian, A. Farag, T. Feeney, D. Baumann, H. Hu, F. Laufer, W. Duan, K. Ding, A. Lambertz, P. Fassl, M. Worgull, U. W. Paetzold, *Adv. Energy Mater.* **2022**, 12, 2200961.

[19] G. Yang, M. Wang, C. Fei, H. Gu, Z. J. Yu, A. Alasfour, Z. C. Holman, J. Huang, *ACS Energy Lett.* **2023**, 8, 1639.

[20] VDMA, *International Technology Roadmap for Photovoltaic*, https://vdma.org.

[21] G. Grancini, C. Roldán-Carmona, I. Zimmermann, E. Mosconi, X. Lee, D. Martineau, S. Narbey, F. Oswald, F. De Angelis, M. Graetzel, M. K. Nazeeruddin, *Nat. Commun.* **2017**, 8, 15684.

[22] A. Mei, Y. Sheng, Y. Ming, Y. Hu, Y. Rong, W. Zhang, S. Luo, G. Na, C. Tian, X. Hou, Y. Xiong, Z. Zhang, S. Liu, S. Uchida, T.-W. Kim, Y. Yuan, L. Zhang, Y. Zhou, H. Han, *Joule* **2020**, 4, 2646.

[23] Y. Kato, L. K. Ono, M. V. Lee, S. Wang, S. R. Raga, Y. Qi, *Adv. Mater. Interfaces* **2015**, 2, 1500195.

[24] J. A. Schwenzer, L. Rakocevic, R. Gehlhaar, T. Abzieher, S. Gharibzadeh, S. Moghadamzadeh, A. Quintilla, B. S. Richards, U. Lemmer, U. W. Paetzold, *ACS Appl. Mater. Interfaces* **2018**, 10, 16390.

[25] D. Zhang, D. Li, Y. Hu, A. Mei, H. Han, *Commun. Mater.* **2022**, 3, 58.

[26] B. Chen, J. Song, X. Dai, Y. Liu, P. N. Rudd, X. Hong, J. Huang, *Adv. Mater.* **2019**, 31, 1902413.

[27] R.-Y. Hsu, Y.-J. Liang, Y.-J. Hung, Y.-C. Lin, *Mater. Sci. Semicond. Process.* **2022**, 152, 107100.

[28] X. Zhang, X. Chen, Y. Chen, N. A. Nadege Ouedraogo, J. Li, X. Bao, C. B. Han, Y. Shirai, Y. Zhang, H. Yan, *Nanoscale Adv.* **2021**, 3, 6128.

[29] M. V. Khenkin, E. A. Katz, A. Abate, G. Bardizza, J. J. Berry, C. Brabec, F. Brunetti, V. Bulović, Q. Burlingame, A. Di Carlo, R. Cheacharoen, Y.-B. Cheng, A. Colsmann, S. Cros, K. Domanski, M. Dusza, C. J. Fell, S. R. Forrest, Y. Galagan, D. Di Girolamo, M. Grätzel, A. Hagfeldt, E. von Hauff, H. Hoppe, J. Kettle, H. Köbler, M. S. Leite, S. Liu, Y.-L. Loo, J. M. Luther, C.-Q. Ma, M. Madsen, M. Manceau, M. Matheron, M. McGehee, R. Meitzner, M. K. Nazeeruddin, A. F. Nogueira, Ç. Odabaşı, A. Osherov, N.-G. Park, M. O. Reese, F. De Rossi, M. Saliba, U. S. Schubert, H. J. Snaith, S. D. Stranks, W. Tress, P. A. Troshin, V. Turkovic, S. Veenstra, I. Visoly-Fisher, A. Walsh, T. Watson, H. Xie, R. Yıldırım, S. M. Zakeeruddin, K. Zhu, M. Lira-Cantu, *Nat. Energy* **2020**, 5, 35.

[30] Z. Ni, H. Jiao, C. Fei, H. Gu, S. Xu, Z. Yu, G. Yang, Y. Deng, Q. Jiang, Y. Liu, Y. Yan, J. Huang, *Nat. Energy* **2022**, 7, 65.

[31] T. A. Chowdhury, M. A. Bin Zafar, M. Sajjad-Ul Islam, M. Shahinuzzaman, M. A. Islam, M. U. Khandaker, *RSC Adv.* **2023**, 13, 1787.

[32] Z. Shen, Q. Han, X. Luo, Y. Shen, Y. Wang, Y. Yuan, Y. Zhang, Y. Yang, L. Han, *Nat. Photonics* **2024**, 18, 450.

[33] F. Gota, R. Schmager, A. Farag, U. W. Paetzold, *Opt. Express* **2022**, 30, 14172.

[34] R. Schmager, M. Langenhorst, J. Lehr, U. Lemmer, B. S. Richards, U. W. Paetzold, *Opt. Express* **2019**, 27, A507.

[35] J. Lehr, M. Langenhorst, R. Schmager, S. Kirner, U. Lemmer, B. S. Richards, C. Case, U. W. Paetzold, *Sustain. Energy Fuels* **2018**, 2, 2754.

[36] R. Schmager, U. W. Paetzold, M. Langenhorst, F. Gota, J. Lehr, https://doi.org/10.5281/ZENODO.4696257 (accessed: May 2024).

[37] M. Remec, Š. Tomšič, M. Khenkin, Q. Emery, J. Li, F. Scheler, B. Glažar, M. Jankovec, M. Jošt, E. Unger, S. Albrecht, R. Schlatmann, B. Lipovšek, C. Ulbrich, M. Topič, *Adv. Energy Mater.* 14, 2304452.

[38] S. Wilcox, W. Marison, *User Manual for TMY3 Dataset*, National Renewable Energy Laboratory, Golden, CO **2008**.

[39] C. A. Gueymard, *Sol. Energy* **2001**, 71, 325.

[40] S. C. Baker-Finch, K. R. McIntosh, *Prog. Photovolt. Res. Appl.* **2011**, 19, 406.

[41] Analog Devices, Inc. LTSpice [Computer software] (n.d.) https://www.analog.com/en/design-center/design-tools-and-calculators/ltspice-simulator.html (accessed May 2024).

[42] M. C. Alonso García, J. L. Balenzategui, *Renew. Energy* **2004**, 29, 1997.

[43] J. T. DuBose, P. V. Kamat, *Mater. Res.* **2022**, 3, 761.

[44] A. F. Gualdrón-Reyes, S. J. Yoon, I. Mora-Seró, *Curr. Opin. Electrochem.* **2018**, 11, 84.

[45] P. Darvishzadeh, G. Redzwan, R. Ahmadi, N. E. Gorji, *Org. Electron.* **2017**, 43, 247.

[46] D. Glowienka, Y. Galagan, *Adv. Mater.* **2022**, 34, 2105920.

[47] C. Xiao, F. Zhang, Z. Li, S. P. Harvey, X. Chen, K. Wang, C.-S. Jiang, K. Zhu, M. Al-Jassim, *Matter* **2020**, 2, 261.

[48] G. Jeong, D. Koo, J. Seo, S. Jung, Y. Choi, J. Lee, H. Park, *Nano Lett.* **2020**, 20, 3718.

[49] H. Zai, Y. Ma, Q. Chen, H. Zhou, *J. Energy Chem.* **2021**, 63, 528.

[50] L. M. Shaker, A. Alamiery, W. N. R. W. Isahak, W. K. Al-Azzawi, *J. Opt.* **2023**.

**ADVANCED
SCIENCE NEWS**

www.advancedsciencenews.com

Energy Technology
Generation, Conversion, Storage, Distribution

www.entechnol.de

[51] E. Köhnen, M. Jošt, A. B. Morales-Vilches, P. Tockhorn, A. Al-Ashouri, B. Macco, L. Kegelmann, L. Korte, B. Rech, R. Schlatmann, B. Stannowski, S. Albrecht, *Sustain. Energy Fuels* **2019**, *3*, 1995.

[52] M. T. Islam, A. Kumar, A. K. Thakur, *J. Electron. Mater.* **2021**, *50*, 3603.

[53] F. Carigiet, C. J. Brabec, F. P. Baumgartner, *Renew. Sustain. Energy Rev.* **2021**, *144*, 111005.

[54] K. Liu, S. Rafique, S. F. Musolino, Z. Cai, F. Liu, X. Li, Y. Yuan, Q. Bao, Y. Yang, J. Chu, X. Peng, C. Nie, W. Yuan, S. Zhang, J. Wang, Y. Pan, H. Zhang, X. Cai, Z. Shi, C. Li, H. Wang, L. Deng, T. Hu, Y. Wang, Y. Wang, S. Chen, L. Shi, P. Ayala, J. E. Wulff, A. Yu, Y. Zhan, *Joule* **2023**, *7*, 1033.

[55] X. Ru, M. Qu, J. Wang, T. Ruan, M. Yang, F. Peng, W. Long, K. Zheng, H. Yan, X. Xu, *Sol. Energy Mater. Sol. Cells* **2020**, *215*, 110643.